Egyptian Journal of Chemistry

http://ejchem.journals.ekb.eg/

Theoretical Calculations and Molecular Design of Novel Quinoline Derivatives as Antibacterial Drugs

Maryam Jamaal Kassar [a] **and Mohammed Oday Ezzat,**[b] *

[a]*Department of Chemistry, College of Education for Pure Sciences, University of Anbar, Ramadi, Anbar, Iraq.*
[b]*Department of Chemistry, College of Education for Women, University of Anbar, Ramadi, Anbar, Iraq*

Abstract

Antibacterial drug efficacy decrease is a consistent problem in both basic and advanced medicine. Every year, approximately 214,000 infants die caused of antibacterial-resistant bacteria. As a consequence, the development of commonly available drugs is essential. For considerations such as high accuracy, reducing time and effort, and high cost, starting from a theoretical chemical study to find alternative treatments is preferable. In this study, 683 Quinoline derivatives are designed and controlled by chemical programs that obey the laws of quantum chemistry and classical mechanics. Molecular-level theory were used. Using Molecular Docking and ΔG, the best 69 Quinoline derivatives were determined. Compounds (H1-H20) showed distinct activity against the New Delhi Metallo-β-Lactamase-1 protein from Klebsiella pneumoniae were H1(ΔG =-8.115). (G1-G20) against Gyrase B from E. coli were G1 (ΔG =-9.611). (W1-W20) against S1:DHFR from Staphylococcus aureus were W1 (ΔG =-8.254). (N1-N20) against Azobenzene from Bacillus subtilis reductase were N1 (ΔG =-6.69). Several compounds have also shown activity against more than one protein like H2 (N15W17). A DFT study was followed to find HOMO (-0.20 to -0.26 eV), LUMO (-0.06 to -0.11 eV), Gap (0.10 to 0.17 eV) for the studied derivatives. These values have been used to determine several molecular properties such as Ionization Potential, Softness and Hardness. Drug-Likeness Predictions (ADME) were applied to show that it obeyed Lipinski's Rule in terms of molecular mass, log *P*, Hydrogen bonding donors, and acceptors. It was found that all the values obtained are within the acceptable values for the use of suggested Quinoline derivatives as medicine.

Keywords: Quinoline Derivatives, Fluoroquinolones, Molecular Docking, DFT study, ADME.

1. Introduction

Antibacterial efficacy, which has revolutionized medicine and saved millions of lives, in jeopardy due to the fast rise of resistant bacteria around the world. It happens when bacteria develop is in the ability to defeat the commercially available drugs to kill them and then continue to grow [1]. As a result, researching novel antibacterial drugs has become a main priority. From the sixties of the last century until now, Quinoline derivatives exhibited a variety of therapeutic and pharmacological activities, including antimalaria, anticancer, antioxidant, anti-inflammatory, and cardiovascular effects, but it is antibacterial activity was unique [2].

Fluoroquinolones (class of Quinoline derivatives) became the most renowned in this field (with the presence of the substituted cyclopropyl and fluorine) against Gram-positive and Gram-negative bacteria at a similar degree. For these considerations, Fluoroquinolones were chosen as a starting point [3]. For a more efficient chemotherapy treatment, several researchers prefer to start with theoretical analysis and molecular design before moving on to the synthesis stage [4]. Computational quantum chemistry can calculate a diverse variety of electronic and thermodynamic parameters that chemists and physicists are interested in. Calculations (based on classical and quantum chemical models) can be used to predict the results of suggested experiments as well as to assist in the interpretation of existing systems. The biological reactions that are catalyzed with enzymes can be simulated by quantum biochemical model that decreases the free energy barrier for binding formation and the binding breaking, also determent the formation of an enzyme active site, as well as equilibrium or nonequilibrium states and light-capturing chromophore. For reactivity of molecules,

*Corresponding author e-mail: edw.mohamed_oday@uoanbar.edu.iq.; (Mohammed Oday Ezzat).
Receive Date: 23 July 2022, Revise Date: 15 August 2022, Accept Date: 30 August 2022.
DOI: 10.21608/EJCHEM.2022.151949.6577

Frontier Orbital Theory (DFT) is a useful method for predicting if aromatic substitutions will experience as electrophilic (electron-poor) or nucleophilic (electron-rich) systems. It provide a better understanding of the complex relationship's nature, but there are some limitations surrounding the use of DFT like complex calculations. For these difficulties and others, many chemical software are developed and each one has its own set of features and a different level of accuracy, intricacy, and accessibility [5].

In this research and to find an effective alternative antibacterial drug; 683 Quinoline derivatives were designed to be theoretically evaluated against four types of bacteria: Bacillus subtilis, Staphylococcus aureus, Escherichia coli and Klebsiella pneumoniae. We hypothesize that these derivatives have a significant binding affinity (ΔG) with specific proteins within these bacteria. Therefore, we simulated the binding affinity between selected proteins and studied derivatives to determine their ability to inhibit the protein and stop its cellular role, and thus reduce bacterial growth. The proteins are: Azobenzene reductase from Bacillus subtilis, S1: Dihydrofolate reductase (S1: DHFR) from Staphylococcus aureus, Gyrase B from E. coli, New Delhi Metallo-β-Lactamase-1 (NDM-1) from Klebsiella pneumoniae. For the simulation, Chem Draw, Chem3D, Gaussian 09, and admetSAR were used for drawing, analyzing and find top binding affinity, DFT (HOMO and LUMO), and determining Structural and electronic properties, as well as, finding in-silico drug-likeness.

2. Computational

Swissdock (a web service) of the Swiss Institute of Bioinformatics – Docking with standard procedure was used to dock the proteins: Azobenzene Reductase from Bacillus subtilis (PDB ID: 1NNI), S1: DHFR from Staphylococcus aureus (PDB ID: 2W9S), Gyrase B from E. coli (PDB ID: 3G7E) and NDM-1 from Klebsiella pneumoniae (PDB ID: 4HL2) with 683 Quinoline derivatives suggested to the active site of proteins. All compounds structures were drawn in ChemOffice (Chem Draw 20.0) with appropriate 2D orientation. MM2 Energy Minimization was estimate for each compound using Chem3D 20.0. MM2 compute steric energy, thermal energy, and other variables, as well as explain how the potential energy surface relates to model conformations [6].

Molecular-level theory is being used. Using the B3LYP/6-31G ++ (d,p) level of theory, the energy-minimized ligand molecules were subsequently subjected to quantum mechanical treatment for geometry optimization and frequency computation. The DFT optimized structures were used as input for Swissdock. From the Protein Data Bank: the crystal structures of receptor molecule 1NNI (Azobenzene Reductase from Bacillus subtilis), 2W9S (Staphylococcus aureus S1:DHFR in complex with trimethoprim), 3G7E (Crystal structure of E. coli Gyrase B co-complexed with PROP-2-YN-1-YL {[5-(4-PIPERIDIN-1-YL-2-PYRIDIN-3-YL-1,3-THIAZOL -5-YL) -1HPYRAZOL -3-YL] METHYL} CARBAMATE inhibitor), and 4HL2 (NDM-1 of Klebsiella pneumoniae) were obtained [7]. Admetsar2 (a web service) were used for in-silico drug-likeness prediction.

3. Results and discussion

Molecular Docking

Docking is a molecular modeling prediction to explain how two or more ligands and proteins fit into each other. It is given by ΔG, A more negative ΔG represents a more suitable binding between compound and protein [8]. ΔG calculations indicated that for 80 compounds as a drug-likeness with anti-bacterial activity were as follows:

- Compounds H1 (N17W10) - H20 have the best activity against *Klebsiella pneumoniae* through their interaction with NDM-1 protein.
- Compounds G1-G20 have the best activity against *E. coli* through their interaction with Gyrase B protein.
- Compounds W1-W20 have the best activity against *Staphylococcus aureus* through their interaction with S1:DHFR protein.
- Compounds N1- N20 (G10) have the best activity against *Bacillus subtilis* through their interaction with Azobenzene Reductase protein.

Compound G1 has the highest binding affinity with protein, ΔG =-9.611, (comparing Ciprofloxacin ΔG = -7.36). Values were also high with W1, ΔG =-8.254, and H1 (N17W10), ΔG =-8.115. Lowest values with non-pathogenic bacteria (Bacillus subtilis) protein by N1, ΔG =-6.69 [9]. Compounds H1 (N17W10), H2 (N15W17), H15 (N7W7) have a significant activity against three bacteria, while five compounds show good activity against two bacteria, which are: H5 (N12), N9 (H14), H10 (G14), G10 (N20), and N10 (H19). Thus, it can be used as a drug in a broader range than other compounds.

Hydrophobic interactions and H-bonding were the most prominent interactions between S1:DHFR and compounds with the participation of residues GLY93, PHE92, ILE5, PHE92, ILE5 and others, as shown in Fig. A.1. Hydrophobic interactions, H-bonding, and polar interactions were the most prominent interactions between GryB and the

compounds with the participation of residues LEU130, LEU132, ILE94, MET95, VAL43, H2O, ASN46, PHE104 and others, as shown in Fig. B.1. π-cation, charge interactions and H-bonding were the most prominent interactions between Azobenzene Reductase and compounds with the participation of residues THR16, GLU73, TYR74, HIE75, SER76 and others, as shown in Fig. C.1. Chelation bonding, H-bonding and Pi-Pi stacking were the most prominent interactions between NDM-1 and compounds with the participation of residues GLN123, LYS211, GLU152, ASN220, divalent ion Zn303, Zn302 and others, as in H2 (N15W17) Fig. D.1. Table 1 illustrates the most prevalent amino acid residues, as well as other molecules and ions that contributed to the protein-compound interactions.

Some derivatives are ranking top 20 binding affinity with more than one protein, their symbol contains the proteins that impact them with their sequence in terms of the binding affinity like N7W7H15, which have great activity against three proteins. as shown in table 2.

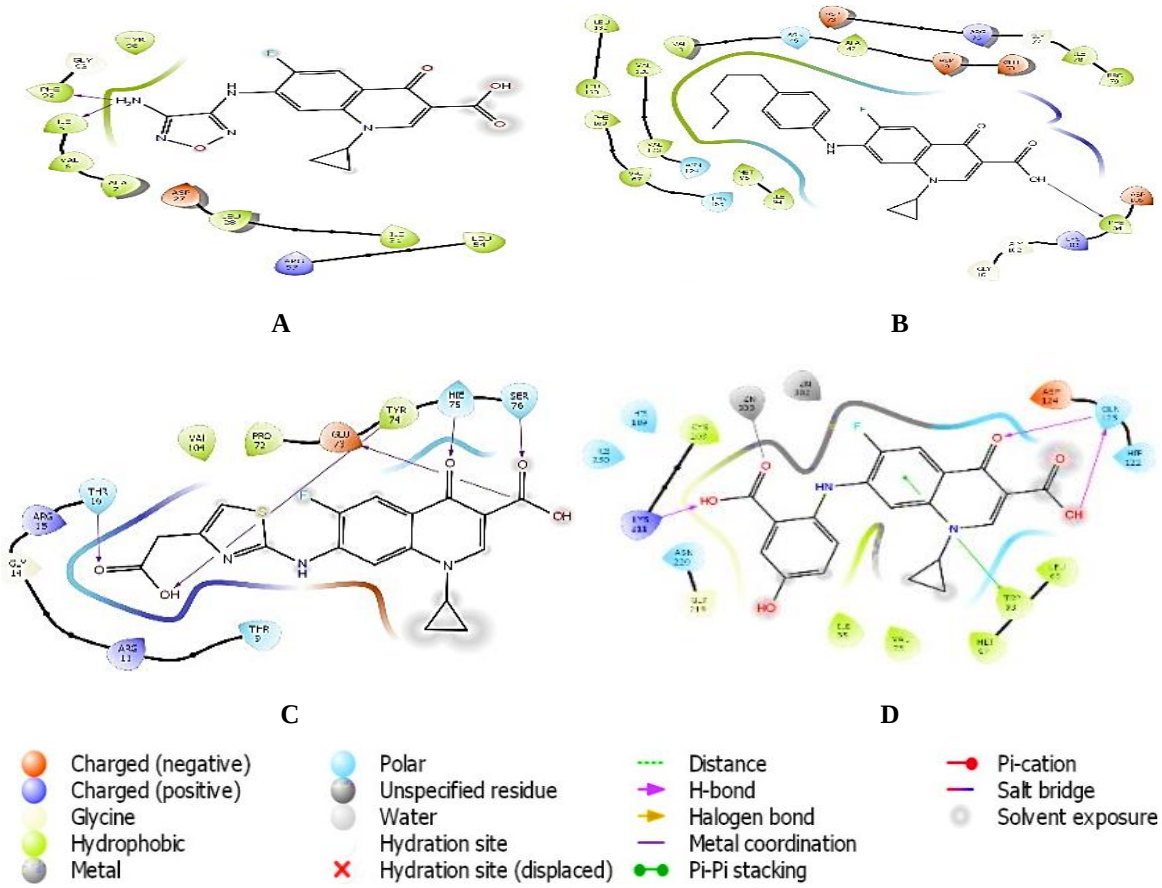

Fig. 1. Protein's interactions with compounds

Table 1. Interactions and Residues relevant of proteins.

proteins	NDM-1	Gyrase B	S1:DHFR	Azobenzene Reductase
Residues relevant	Zn303, Zn302 (Chelation bonding), GLN123 & LYS211 & GLU152 & ASN220 (H-bonding), TRP93 & HIE122& HIS250 (π-π stacking).	VAL123,120,43,167 & PHE169 & MET95 & ILE78,94 & PRO79 (Hydrophobic interactions), PHE104 & ASN46 (H-bonding), ASP49,73 & ASN46 (Polar interactions).	GLY93 & PHE92 & ILE5,50,31 &LEU28 & VAL6 & ALA7 (Hydrophobic interactions), ASP27 & LEU20 & H2O &PHE92 & ILE5 (H-bonding).	ARG11 &ARG15 (charge interactions), ARG11 (π - cation), THR16 & GLU73 & TYR74 & HIE75 & SER76 (H-bonding).

Table (2) Chemical structure and ΔG of the studied compounds

Core	Azobenzene Reductase from *B.subtilis* (1NNI)	*Staphylococcus aureus* S1:DHFR (2W9S)	*E. coli* Gyrase B (3G7E)	New Delhi Metallo-beta-Lactamase-1 (4HL2)
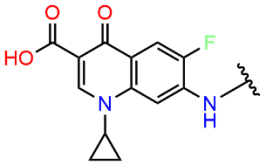	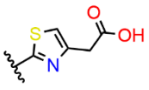 N1 ΔG =-6.69	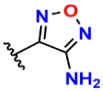 W1 ΔG =-8.254	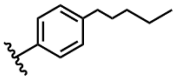 G1 ΔG =-9.611	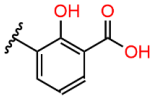 H1N17W10 ΔG =-8.115
	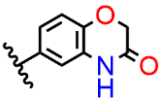 N2 ΔG =-6.423	 W2 ΔG =-7.875	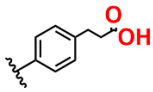 G2 ΔG =-9.466	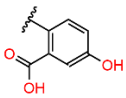 H2N15W17 ΔG =-7.966
	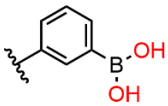 N3 ΔG =-6.357	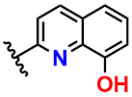 W3 ΔG =-7.836	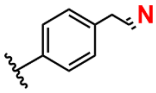 G3 ΔG =-9.362	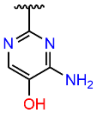 H3 ΔG =-7.832
	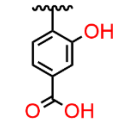 N4 ΔG =-6.259	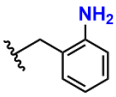 W4 ΔG =-7.734	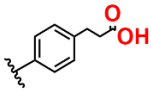 G4 ΔG =-9.087	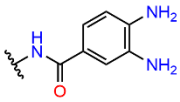 H4 ΔG =-7.647
	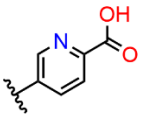 N5 ΔG =-6.158	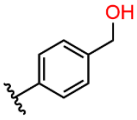 W5 ΔG =-7.723	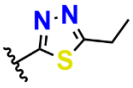 G5 ΔG =-8.992	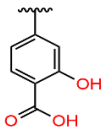 H5N12 ΔG =-7.61
	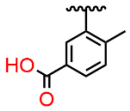 N6 ΔG =-6.152	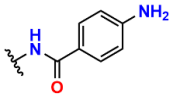 W6 ΔG =-7.664	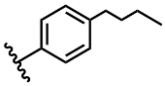 G6 ΔG =-8.819	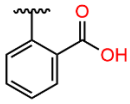 H6 ΔG =-7.599
	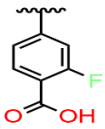 N7W7H15 ΔG =-6.063	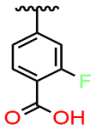 W7N7H15 ΔG =-7.658	 G7 ΔG =-8.771	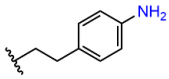 H7 ΔG =-7.487
	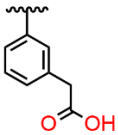 N8 ΔG =-6.032	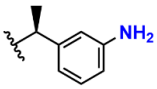 W8 ΔG =-7.582	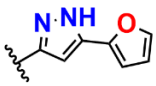 G8 ΔG =-8.747	 H8 ΔG =-7.451

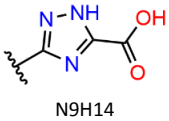 N9H14 ΔG =-5.891	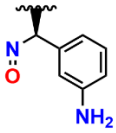 W9 ΔG =-7.483	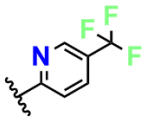 G9 ΔG =-8.73	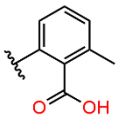 H9 ΔG =-7.445
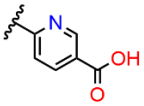 N10H19 ΔG =-5.702	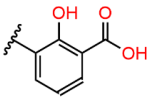 W10N17H1 ΔG =-7.364	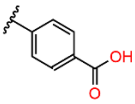 G10N20 ΔG =-8.667	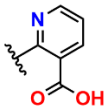 H10G14 ΔG =-7.425
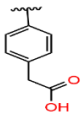 N11 ΔG =-5.674	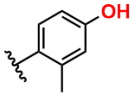 W11 ΔG =-7.309	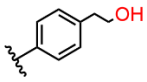 G11 ΔG =-8.61	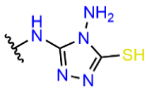 H11 ΔG =-7.418
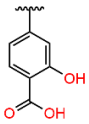 N12H5 ΔG =-5.356	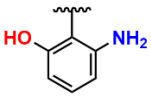 W12 ΔG =-7.305	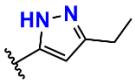 G12 ΔG =-8.566	 H12 ΔG =-7.394
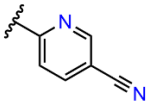 N13 ΔG =-5.331	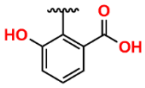 W13 ΔG =-7.288	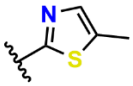 G13 ΔG =-8.532	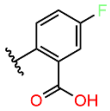 H13 ΔG =-7.376
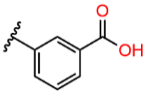 N14 ΔG =-5.26	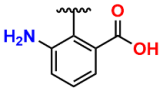 W14 ΔG =-7.286	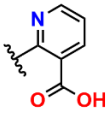 G14H10 ΔG =-8.529	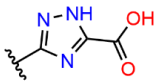 H14N9 ΔG = -7.371
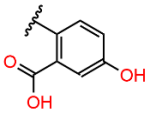 N15W17H2 ΔG =-5.211	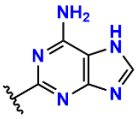 W15 ΔG =-7.232	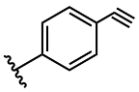 G15 ΔG =-8.515	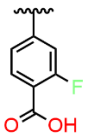 H15N7W7 ΔG = -7.368
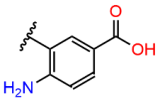 N16 ΔG =-5.172	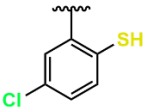 W16 ΔG =-7.229	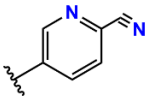 G16 ΔG =-8.489	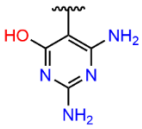 H16 ΔG = -7.356
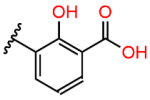 N17H1W10 ΔG =-5.138	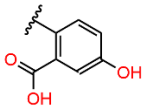 W17N15H2 ΔG =-7.223	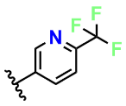 G17 ΔG =-8.471	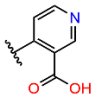 H17 ΔG = -7.351

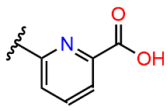 N18 ΔG =-5.092	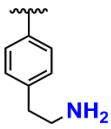 W18 ΔG =-7.215	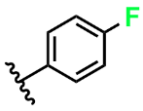 G18 ΔG =-8.409	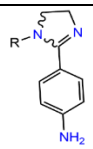 H18 ΔG = -7.345
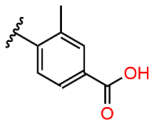 N19 ΔG =-5.082	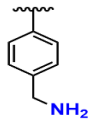 W19 ΔG =-7.206	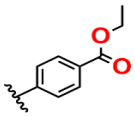 G19 ΔG =-8.408	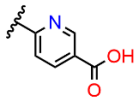 H19N10 ΔG = -7.325
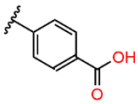 N20 ΔG =-5.063	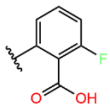 W20 ΔG =-7.203	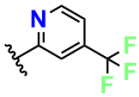 G20 ΔG =-8.385	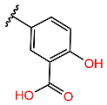 H20 ΔG = -7.306

DFT Analysis

DFT, Density-functional theory, is an atomistic simulation calculating to find a wide range of important properties such as HOMOs are the highest occupied molecular orbitals, and LUMOs is the lowest lying unoccupied molecular orbitals, and the Gap between them in the molecular-level theory. This simulation predicts that a site where the LUMO is localized, is a good electrophilic site. So LUMO's value link to electron affinity. Similarly, that a site where the HOMO's is localized, is electrons most free to participate in the interactions. So ionization potential affects by HOMO's value. HOMO, LUMO and GAP measurements confirmed the tendency of molecules to behave as acids rather than bases, as well as molecules have great kinetic activity but low stability. The Figure (3.24) shown the HOMO and LUMO in G1, W1, H1 (N17W10), N1 HOMO values of all compound ranged from -0.20 to -0.26 eV, LUMO's values were -0.06 to -0.11 eV and the Gap were 0.10 to 0.17 eV. these features were employed in equations to find many molecular properties such ionization potential (I) and electron affinity EA:

$$I = -E_{HOMO} \quad \ldots(1),$$

$$EA = -E_{LUMO} \ldots(2)$$

The values of the studied compounds ranged (0.202- 0.252) to the I, and ranged from (0.063 - 0.116) to the EA. To Electronegativity (μ), softness (S), Hardness (η), and index global electrophilicity (ω) finding, the equations (3),(4),(5), and (6) were used:

$$\mu = -\frac{1}{2}(E_{HOMO} + E_{LUMO}) \ldots (3)$$

$$(S) = -\frac{2}{(E_{HOMO} - E_{LUMO})} \quad \ldots(4)$$

$$\eta = -\frac{1}{2}(E_{HOMO} - E_{LUMO}) \quad \ldots (5)$$

$$(\omega) = \frac{\mu 2}{2\eta} \quad \ldots(6)$$

Where the values were between (0.138- 0.173) for Electronegativity, between (12.31- 18.66) for softness, between (0.053-0.081) Hardness, and between (0.008- 0.013) for index global electrophilicity [11].

In-silico Drug-Likeness Predictions

Drug-likeness criteria are a set of standards for the structural properties of compounds that may be used to quickly calculate a molecule's drug-like qualities according to 'Lipinski's rule, before the compound is ever synthesized and evaluated. The five-parameter is a guideline for determining if a chemical molecule with a certain biological activity has qualities that would make it a likely orally active medication in humans. Where the drug must not violate more than one of the criteria related to molecular mass, log *P*, hydrogen-bond donors and acceptors.

For the 69 compounds, molecular mass were (356.33-411.39) when the domain between (86-829), log p were (1.6- 5.65) the domain (-23.7-8.3), H-bond donors were (2-5) domain (under 7), H-bond acceptors

were (5-10), domain (under 15). These indicates that all of the values are within an acceptable ranges [12].

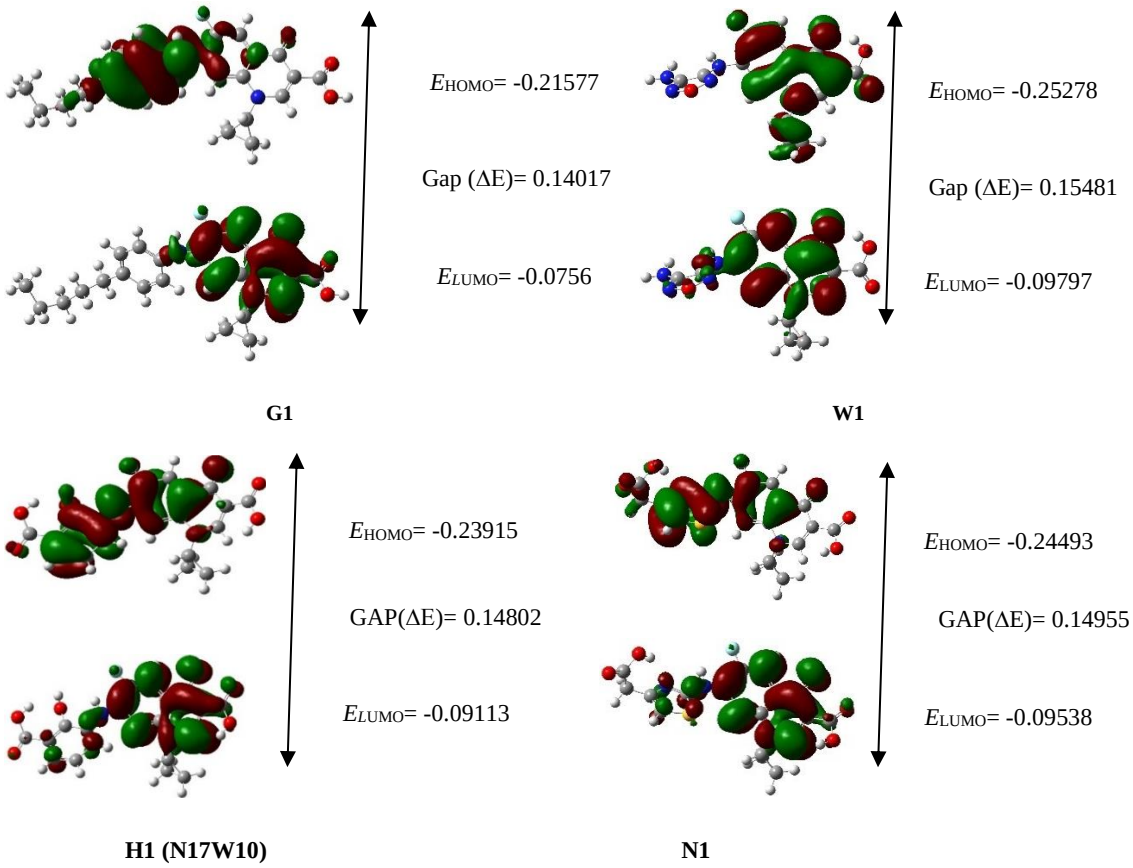

Fig (3-24): HOMO, LUMO and Gap for G1, W1, H1 (N17W10) and N1.

Human oral bioavailability (HOB)

Bioavailability refers to the rate and extent to which the Active Pharmaceutical Ingredient (API) is accessible at the target site. This is the closest thing to identifying a medicine's "optimal" bioavailability. The letter F stands for the fraction of the active drug that remains unchanged in the systemic circulation, The calculation is built on the presumption that the concentration of drug in blood or plasma is proportional to its concentration at the action site. Similarly, the compounds were classified based on their percent F values (F% ≤ 50% as "reduced," F% ≥ 50% as "high").

The bioavailability of N1-N20 (G10) quinolones ranged from 78% to 92%, W1-W20 quinolones from 71% to 89%, G1-G20 quinolones from 71% to 92%, and H1 (N17W10) -H20 quinolones from 70% to 92%. All of the results are shown in, which is considered high based on the F% values, that were greater than 50%.

Human Intestinal Absorption (HIA)

One of the most relevant ADMET features is human intestinal absorption, it's also an important stage in the delivery of pharmaceuticals to their intended recipients. Various processes deliver drug molecules from the gastroenteric system to the blood circulation and allow them to pass through the gastroenteric membrane. Passive diffusion is the principal process, which is induced by a concentration difference. P-Glycoprotein (P-gp) is a common carrier of pharmaceuticals through the intestine, causing efflux[95]. HIA was categorized into three parts: high (100–67%), middle (66–33%), and low (32–0%)[96]. The HIA values for all of the quinolones examined ranged from 87% to 96%, which is a high percentage, as seen by the HIA values.

Table (3) Chemical properties of studied compounds.

1. Comp.	2. N1	3. N2	4. N3	5. N4	6. N5	7. N6	8. N7	9. N8	10. N9	11. N10
12. LUMO	13. -0.095	14. -0.084	15. -0.085	16. -0.089	17. -0.094	18. -0.089	19. -0.076	20. -0.083	21. -0.089	22. -0.084
23. HOMO	24. -0.245	25. -0.215	26. -0.236	27. -0.237	28. -0.225	29. -0.243	30. -0.236	31. -0.237	32. -0.234	33. -0.241
34. GAP	35. 0.15	36. 0.13	37. 0.152	38. 0.147	39. 0.13	40. 0.154	41. 0.16	42. 0.154	43. 0.145	44. 0.157
45. IP/ eV	46. 0.245	47. 0.215	48. 0.236	49. 0.237	50. 0.225	51. 0.243	52. 0.236	53. 0.237	54. 0.234	55. 0.241
56. EA/ eV	57. 0.095	58. 0.084	59. 0.085	60. 0.089	61. 0.094	62. 0.089	63. 0.076	64. 0.083	65. 0.089	66. 0.084
67. (μ) χ	68. 0.17	69. 0.15	70. 0.161	71. 0.163	72. 0.159	73. 0.166	74. 0.156	75. 0.16	76. 0.161	77. 0.163
78. η	79. 0.075	80. 0.065	81. 0.076	82. 0.074	83. 0.065	84. 0.077	85. 0.08	86. 0.077	87. 0.072	88. 0.079
89. S	90. 13.37	91. 15.33	92. 13.18	93. 13.59	94. 15.37	95. 12.97	96. 12.51	97. 13.02	98. 13.83	99. 12.74
100. (ω)	101. 0.013	102. 0.01	103. 0.012	104. 0.012	105. 0.01	106. 0.013	107. 0.012	108. 0.012	109. 0.012	110. 0.013
111. Redox potential	112. 2.568	113. 2.545	114. 2.793	115. 2.646	116. 2.378	117. 2.737	118. 3.097	119. 2.849	120. 2.624	121. 2.869

122.

123. Comp.	124. N11	125. N12	126. N13	127. N14	128. N15	129. N16	130. N17	131. N18-H3	132. N19	133. N20
134. LUMO	135. -0.094	136. -0.098	137. -0.097	138. -0.088	139. -0.087	140. -0.085	141. -0.093	142. -0.086	143. -0.08	144. -0.077
145. HOMO	146. -0.244	147. -0.24	148. -0.251	149. -0.229	150. -0.246	151. -0.241	152. -0.238	153. -0.244	154. -0.224	155. -0.239
156. GAP	157. 0.15	158. 0.142	159. 0.154	160. 0.141	161. 0.159	162. 0.156	163. 0.145	164. 0.158	165. 0.143	166. 0.162
167. IP/ eV	168. 0.244	169. 0.24	170. 0.251	171. 0.229	172. 0.246	173. 0.241	174. 0.238	175. 0.244	176. 0.224	177. 0.239
178. EA/ eV	179. 0.094	180. 0.098	181. 0.097	182. 0.088	183. 0.087	184. 0.085	185. 0.093	186. 0.086	187. 0.08	188. 0.077
189. (μ) χ	190. 0.169	191. 0.169	192. 0.174	193. 0.158	194. 0.166	195. 0.163	196. 0.166	197. 0.165	198. 0.152	199. 0.158
200. η	201. 0.075	202. 0.071	203. 0.077	204. 0.071	205. 0.079	206. 0.078	207. 0.072	208. 0.079	209. 0.072	210. 0.081
211. S	212. 13.37	213. 14.1	214. 12.97	215. 14.14	216. 12.61	217. 12.83	218. 13.82	219. 12.66	220. 13.97	221. 12.34
222. (ω)	223. 0.013	224. 0.012	225. 0.013	226. 0.011	227. 0.013	228. 0.013	229. 0.012	230. 0.013	231. 0.011	232. 0.013
233. Redox potential	234. 2.589	235. 2.448	236. 2.591	237. 2.612	238. 2.823	239. 2.835	240. 2.55	241. 2.829	242. 2.782	243. 3.107

244.

245. Comp.	246. W1	247. W2	248. W3	249. W4	250. W5	251. W6	252. W7	253. W8	254. W9	255. W10
256. LUMO	257. -0.098	258. -0.091	259. -0.076	260. -0.065	261. -0.089	262. -0.072	263. -0.094	264. -0.079	265. -0.072	266. -0.116
267. HOMO	268. -0.253	269. -0.217	270. -0.218	271. -0.221	272. -0.229	273. -0.223	274. -0.247	275. -0.219	276. -0.233	277. -0.223
278. GAP	279. 0.155	280. 0.126	281. 0.142	282. 0.156	283. 0.14	284. 0.151	285. 0.153	286. 0.14	287. 0.161	288. 0.107
289. IP/ eV	290. 0.253	291. 0.217	292. 0.218	293. 0.221	294. 0.229	295. 0.223	296. 0.247	297. 0.219	298. 0.233	299. 0.223
300. EA/ eV	301. 0.098	302. 0.091	303. 0.076	304. 0.065	305. 0.089	306. 0.072	307. 0.094	308. 0.079	309. 0.072	310. 0.116
311. (μ) χ	312. 0.175	313. 0.154	314. 0.147	315. 0.143	316. 0.159	317. 0.147	318. 0.171	319. 0.149	320. 0.153	321. 0.17
322. η	323. 0.077	324. 0.063	325. 0.071	326. 0.078	327. 0.07	328. 0.075	329. 0.076	330. 0.07	331. 0.08	332. 0.054
333. S	334. 12.92	335. 15.89	336. 14.08	337. 12.86	338. 14.24	339. 13.26	340. 13.1	341. 14.32	342. 12.43	343. 18.67
344. (ω)	345. 0.014	346. 0.01	347. 0.01	348. 0.011	349. 0.011	350. 0.011	351. 0.013	352. 0.01	353. 0.012	354. 0.009
355. Redox potential	356. 2.58	357. 2.376	358. 2.88	359. 3.38	360. 2.581	361. 3.103	362. 2.619	363. 2.764	364. 3.233	365. 1.922

366. Comp.	367. W11	368. W12	369. W13	370. W14	371. W15	372. W16	373. W17	374. W18	375. W19	376. W20
377. LUMO	378. -0.073	379. -0.083	380. -0.075	381. -0.064	382. -0.083	383. -0.071	384. -0.08	385. -0.083	386. -0.072	387. -0.09
388. HOMO	389. -0.223	390. -0.202	391. -0.228	392. -0.222	393. -0.212	394. -0.22	395. -0.233	396. -0.221	397. -0.214	398. -0.226
399. GAP	400. 0.15	401. 0.12	402. 0.153	403. 0.158	404. 0.129	405. 0.149	406. 0.153	407. 0.138	408. 0.142	409. 0.136
410. IP/ eV	411. 0.223	412. 0.202	413. 0.228	414. 0.222	415. 0.212	416. 0.22	417. 0.233	418. 0.221	419. 0.214	420. 0.226
421. EA/ eV	422. 0.073	423. 0.083	424. 0.075	425. 0.064	426. 0.083	427. 0.071	428. 0.08	429. 0.083	430. 0.072	431. 0.09
432. (μ) χ	433. 0.148	434. 0.142	435. 0.152	436. 0.143	437. 0.148	438. 0.146	439. 0.156	440. 0.152	441. 0.143	442. 0.158

443. η	444. 0.075	445. 0.06	446. 0.076	447. 0.079	448. 0.065	449. 0.075	450. 0.077	451. 0.069	452. 0.071	453. 0.068
454. S	455. 13.33	456. 16.71	457. 13.07	458. 12.62	459. 15.47	460. 13.4	461. 13.04	462. 14.52	463. 14.08	464. 14.73
465. (ω)	466. 0.011	467. 0.009	468. 0.012	469. 0.011	470. 0.01	471. 0.011	472. 0.012	473. 0.01	474. 0.01	475. 0.011
476. Redox potential	477. 3.06	478. 2.448	479. 3.03	480. 3.478	481. 2.558	482. 3.104	483. 2.928	484. 2.657	485. 2.964	486. 2.507

487. Comp.	488. G1	489. G2	490. G3	491. G4	492. G5	493. G6	494. G7	495. G8	496. G9	497. G10
498. LUMO	499. -0.076	500. -0.079	501. -0.081	502. -0.076	503. -0.084	504. -0.076	505. -0.078	506. -0.072	507. -0.078	508. -0.079
509. HOMO	510. -0.216	511. -0.224	512. -0.235	513. -0.216	514. -0.243	515. -0.216	516. -0.22	517. -0.231	518. -0.241	519. -0.232
520. GAP	521. 0.14	522. 0.145	523. 0.154	524. 0.14	525. 0.159	526. 0.14	527. 0.143	528. 0.16	529. 0.162	530. 0.153
531. IP/ eV	532. 0.216	533. 0.224	534. 0.235	535. 0.216	536. 0.243	537. 0.216	538. 0.22	539. 0.231	540. 0.241	541. 0.232
542. EA/ eV	543. 0.076	544. 0.079	545. 0.081	546. 0.076	547. 0.084	548. 0.076	549. 0.078	550. 0.072	551. 0.078	552. 0.079
553. (μ) χ	554. 0.146	555. 0.151	556. 0.158	557. 0.146	558. 0.164	559. 0.146	560. 0.149	561. 0.151	562. 0.159	563. 0.155
564. η	565. 0.07	566. 0.072	567. 0.077	568. 0.07	569. 0.079	570. 0.07	571. 0.071	572. 0.08	573. 0.081	574. 0.077
575. S	576. 14.27	577. 13.8	578. 12.98	579. 14.28	580. 12.59	581. 14.32	582. 14	583. 12.53	584. 12.32	585. 13.05
586. (ω)	587. 0.01	588. 0.011	589. 0.012	590. 0.01	591. 0.013	592. 0.01	593. 0.011	594. 0.012	595. 0.013	596. 0.012
597. Redox potential	598. 2.854	599. 2.837	600. 2.913	601. 2.847	602. 2.887	603. 2.835	604. 2.841	605. 3.228	606. 3.076	607. 2.951

608. Comp.	609. G11	610. G12	611. G13	612. G14	613. G15	614. G16	615. G17	616. G18	617. G19	618. G20
619. LUMO	620. -0.077	621. -0.077	622. -0.08	623. -0.089	624. -0.08	625. -0.098	626. -0.086	627. -0.079	628. -0.079	629. -0.092
630. HOMO	631. -0.223	632. -0.226	633. -0.224	634. -0.247	635. -0.223	636. -0.25	637. -0.247	638. -0.227	639. -0.228	640. -0.251
641. GAP	642. 0.146	643. 0.148	644. 0.144	645. 0.159	646. 0.143	647. 0.152	648. 0.161	649. 0.149	650. 0.149	651. 0.159
652. IP/ eV	653. 0.223	654. 0.226	655. 0.224	656. 0.247	657. 0.223	658. 0.25	659. 0.247	660. 0.227	661. 0.228	662. 0.251
663. EA/ eV	664. 0.077	665. 0.077	666. 0.08	667. 0.089	668. 0.08	669. 0.098	670. 0.086	671. 0.079	672. 0.079	673. 0.092
674. (μ) χ	675. 0.15	676. 0.152	677. 0.152	678. 0.168	679. 0.152	680. 0.174	681. 0.166	682. 0.153	683. 0.154	684. 0.171
685. η	686. 0.073	687. 0.074	688. 0.072	689. 0.079	690. 0.071	691. 0.076	692. 0.081	693. 0.074	694. 0.075	695. 0.08
696. S	697. 13.71	698. 13.48	699. 13.87	700. 12.61	701. 14	702. 13.13	703. 12.41	704. 13.45	705. 13.38	706. 12.57
707. (ω)	708. 0.011	709. 0.011	710. 0.011	711. 0.013	712. 0.011	713. 0.013	714. 0.013	715. 0.011	716. 0.011	717. 0.014
718. Redox potential	719. 2.885	720. 2.916	721. 2.805	722. 2.787	723. 2.779	724. 2.555	725. 2.877	726. 2.894	727. 2.894	728. 2.734

729. Comp.	730. H1	731. H2	732. H3	733. H4	734. H5	735. H6	736. H7	737. H8	738. H9	739. H10
740. LUMO	741. -0.091	742. -0.08	743. -0.083	744. -0.071	745. -0.076	746. -0.087	747. -0.085	748. -0.069	749. -0.073	750. -0.094
751. HOMO	752. -0.239	753. -0.227	754. -0.236	755. -0.218	756. -0.204	757. -0.231	758. -0.236	759. -0.207	760. -0.203	761. -0.245
762. GAP	763. 0.148	764. 0.148	765. 0.153	766. 0.148	767. 0.128	768. 0.144	769. 0.151	770. 0.138	771. 0.13	772. 0.151
773. IP/ eV	774. 0.239	775. 0.227	776. 0.236	777. 0.218	778. 0.204	779. 0.231	780. 0.236	781. 0.207	782. 0.203	783. 0.245
784. EA/ eV	785. 0.091	786. 0.08	787. 0.083	788. 0.071	789. 0.076	790. 0.087	791. 0.085	792. 0.069	793. 0.073	794. 0.094
795. (μ) χ	796. 0.165	797. 0.154	798. 0.16	799. 0.145	800. 0.14	801. 0.159	802. 0.161	803. 0.138	804. 0.138	805. 0.169
806. η	807. 0.074	808. 0.074	809. 0.076	810. 0.074	811. 0.064	812. 0.072	813. 0.075	814. 0.069	815. 0.065	816. 0.075
817. S	818. 13.51	819. 13.54	820. 13.1	821. 13.55	822. 15.6	823. 13.93	824. 13.25	825. 14.49	826. 15.38	827. 13.28
828. (ω)	829. 0.012	830. 0.011	831. 0.012	832. 0.011	833. 0.009	834. 0.011	835. 0.012	836. 0.01	837. 0.009	838. 0.013
839. Redox potential	840. 2.624	841. 2.853	842. 2.83	843. 3.083	844. 2.685	845. 2.652	846. 2.766	847. 2.989	848. 2.778	849. 2.6

850. Comp.	851. H11	852. H12	853. H13	854. H14	855. H15	856. H16	857. H17	858. H18	859. H19	860. H20
861. LUMO	862. -0.084	863. -0.088	864. -0.079	865. -0.068	866. -0.092	867. -0.09	868. -0.086	869. -0.094	870. -0.076	871. -0.095
872. HOMO	873. -0.243	874. -0.231	875. -0.236	876. -0.226	877. -0.253	878. -0.235	879. -0.235	880. -0.237	881. -0.205	882. -0.248

883. GAP	884. 0.158	885. 0.143	886. 0.157	887. 0.158	888. 0.16	889. 0.145	890. 0.149	891. 0.143	892. 0.129	893. 0.153
894. IP/ eV	895. 0.243	896. 0.231	897. 0.236	898. 0.226	899. 0.253	900. 0.235	901. 0.235	902. 0.237	903. 0.205	904. 0.248
905. EA/ eV	906. 0.084	907. 0.088	908. 0.079	909. 0.068	910. 0.092	911. 0.09	912. 0.086	913. 0.094	914. 0.076	915. 0.095
916. (μ) χ	917. 0.164	918. 0.159	919. 0.158	920. 0.147	921. 0.173	922. 0.162	923. 0.161	924. 0.166	925. 0.14	926. 0.171
927. η	928. 0.079	929. 0.072	930. 0.079	931. 0.079	932. 0.08	933. 0.072	934. 0.074	935. 0.072	936. 0.064	937. 0.076
938. S	939. 12.62	940. 13.98	941. 12.7	942. 12.66	943. 12.5	944. 13.81	945. 13.46	946. 13.94	947. 15.55	948. 13.1
949. (ω)	950. 0.013	951. 0.011	952. 0.012	953. 0.012	954. 0.014	955. 0.012	956. 0.012	957. 0.012	958. 0.009	959. 0.013
960. Redox potential	961. 2.876	962. 2.63	963. 2.994	964. 3.31	965. 2.731	966. 2.609	967. 2.719	968. 2.528	969. 2.695	970. 2.608

5. Conclusions

The 69 proposed fluoroquinolones showed significant theoretically activity against Bacillus subtilis, Staphylococcus aureus, E. coli and Klebsiella pneumoniae.The compound G1 has the highest binding affinity with gyrase B (compared with Ciprofloxacin ΔG = -7.36), Hence a good activity against E.coli bacteria. Compounds H1 (N17W10), H2 (N15W17), H15 (N7W7) have significant activity against three bacteria, While five compounds show good activity against two bacteria. Thus, it can be used as a drug in a broader range than other compounds.The calculated chemical properties (such as molecular weight, log *p*, ionization energy, electronic affinity, donating or accepting hydrogen bonds, etc.) indicate that these molecules have unique therapeutic properties that can be employed to overcome the problem of bacterial resistance.

6. References

[1] Ventola, C. L. (2015) 'The Antibiotic Resistance Crisis: Part 1: Causes and Threats', Pharmacy and Therapeutics, 40(4), p. 277. doi: Article.

[2] Matada, B. S., Pattanashettar, R. and Yernale, N. G. (2021) 'A comprehensive review on the biological interest of quinoline and its derivatives', Bioorganic & Medicinal Chemistry, 32, p. 115973. doi: 10.1016/J.BMC.2020.115973.

[3] Abbaz, T., Bendjeddou, A. and Villemin, D. (2019) 'Theoretical Analysis and Molecular Orbital studies of Sulfonamides Products with N-Alkylation and O-alkylation', *International Journal of Advanced Engineering Research and Science*, 6(2), pp. 91–101. doi: 10.22161/IJAERS.6.2.12.

[4] Yankova, R. et al. (2016) 'Molecular structure, vibrational spectra, MEP, HOMO-LUMO and NBO analysis of Hf(SeO3)(SeO4)(H2O)4', Journal of Molecular Structure, 1106, pp. 82–88. doi: 10.1016/J.MOLSTRUC.2015.10.091.

[5] Simón, L. and Paton, R. S. (2016) 'QM/MM study on the enantioselectivity of spiroacetalization catalysed by an imidodiphosphoric acid catalyst: How confinement works', *Organic and Biomolecular Chemistry*, 14(11), pp. 3031–3039. doi: 10.1039/C6OB00045B.

[6] Shi, Y. and Szlufarska, I. (2020) 'Wear-induced microstructural evolution of nanocrystalline aluminum and the role of zirconium dopants', Acta Materialia, 200, pp. 432–441. doi: 10.1016/J.ACTAMAT.2020.09.005.

[7] Salihović, M. *et al.* (2014) 'DFT study and biological activity of some methylxanthines', *Bull. Chem. Technol. Bosnia Herzeg*, 42(c), pp. 31–36.

[8] Meng, X.-Y. *et al.* (2011) 'Molecular Docking: A powerful approach for structure-based drug discovery', *Current computer-aided drug design*, 7(2), p. 146. doi: 10.2174/157340911795677602.

[9] Al-Karmalawy, A. A. *et al.* (2021) 'Molecular Docking and Dynamics Simulation Revealed the Potential Inhibitory Activity of ACEIs Against SARS-CoV-2 Targeting the hACE2 Receptor', *Frontiers in Chemistry*, 9, p. 227. doi: 10.3389/FCHEM.2021.661230/BIBTEX.

[10] Kumer, A., Sarker, M. N. and Paul, S. (2019) 'The theoretical investigation of HOMO, LUMO, thermophysical properties and QSAR study of some aromatic carboxylic acids using HyperChem programming', *International Journal of Chemistry and Technology*, 3(1), pp. 26–37. doi: 10.32571/ijct.478179.

[11] Sens, L. *et al.* (2018) 'Synthesis, antioxidant activity, acetylcholinesterase inhibition and quantum studies of thiosemicarbazones', *Journal of the Brazilian Chemical Society*, 29(2), pp. 343–352. doi: 10.21577/0103-5053.20170146.

[12] Tian, S. *et al.* (2015) 'The application of in silico drug-likeness predictions in pharmaceutical research', *Advanced Drug Delivery Reviews*, 86, pp. 2–10. doi: 10.1016/J.ADDR.2015.01.009.